A STUDY ON STRUCTURAL PERFORMANCE CONSIDERING CONNECTING CONDITION OF PILLAR TYPE HYSTERETIC DAMPERS FOR R/C BUILDINGS

Tsunehisa MATSUURA[1], Eiichi INAI[2] and Toshiaki FUJIMOTO[3]

[1] *Technical Research Institute, HAZAMA Corp., Ibaraki. Japan*
[2] *Professor, Graduate School of Science and Engineering, Yamaguchi Univ., Yamaguchi. Japan*
[3] *ANDO Corporation Research Center, Saitama. Japan*
Email: matsuura@hazama.co.jp, inai@yamaguchi-u.ac.jp, fujimoto-toshiaki@ando-corp.co.jp

ABSTRACT :

In this research, a structural experiment was conducted on a pillar type hysteretic damper applied to a reinforced concrete (RC) building using as a parameter the method of connecting the damper to the reinforced concrete at the base of the damper. Based on the test results, the effects of the joint method on the deformation components in the RC support, load transfer mechanism and the hysteresis characteristics were identified. It was revealed that the building construction using a proposed simple method of joint enables damper performance to develop fully.

KEYWORDS: reinforced concrete,hysteretic damper,encased in R/C base,load transfer mechanism

1. INTRODUCTION

Seismic control technology, which has been applied mainly to steel framed buildings, has recently been adopted in high-rise RC buildings in an increasing number of cases. RC buildings have much greater lateral stiffness that steel framed buildings. Energy dissipation devices have been applied to RC structures should therefore be designed to minimize relative story displacement at yielding. To that end, adequate stiffness should be provided at the position where the energy dissipation device is installed to concentrate deformation at the damper. Building plans, however, show that only limited space is available for installing energy dissipation members. The size of the support of the energy dissipation devices attached should be minimized, so securing adequate stiffness is difficult.

A new method was developed for linking a pillar type steel hysteretic damper with its top and bottom encased in RC (Fig.1) to building frame. It is more effective than existing methods [1], [2].

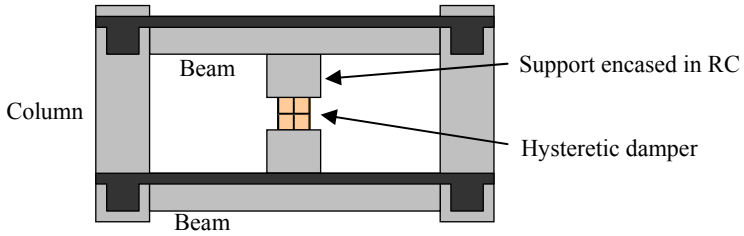

Figure 1 Outline of pillar type steel hysteretic damper

2. SIGNIFICANCE OF RESEARCH

In order to apply steel hysteretic dampers to RC structures, it is necessary to encase the supports of the energy dissipation devices in RC to concentrate deformation at the damper and reinforce the performance of the damper. The RC encasing the supports of the damper should be provided with adequate strength and stiffness to transmit

the bearing capacity of the damper to the beams of the frame. Damage to the reinforced concrete due to cracking is, however, inevitable. Identifying the load transfer mechanism and the hysteresis characteristics are extremely important to the evaluation of the performance of pillar type dampers.

This research focused on the structural performance of the joint between the steel hysteretic damper and the support of damper encased in RC. In the experiment of elements, loading tests were conducted focused on the behavior of supports of damper encased in RC using specimens with various joint characteristics. The objective was to identify the load transfer mechanism and the hysteresis characteristics in the RC support. Then, in the experiment of members, verification was made for the entire device composed of a steel damper with low-yield-strength steel using the joint method that was found most effective in the element test. This paper outlines the structural experiments and describes the load transfer mechanism.

3. EXPERIMENTAL PROGRAM

3.1. Details of specimens and materials

Table 1 lists specimens and Fig. 2 shows the shapes of specimens. The cross section of RC support around the base of the damper and the embedment depth of steel were set at the same level for all the specimens. The cross-sectional area was set at 300 (B) x 500 (D) mm and the embedment depth of steel at 300 mm, the depth of H-section steel. The main reinforcement used in the RC support around the base of the damper was 18-D16 (diameter: 16 mm, yield stress: 444 MPa) in specimen No. 1 through 3, 12-D16 (yield stress: 451 MPa) in specimen No. 4 through 6, 16-D16 (yield stress: 374 MPa) in specimen No. 7 and 20-D16 (yield stress: 374 MPa) in specimen No. 8. Mechanical anchorage was adopted for all the main reinforcement except the one in specimen No. 2. In the RC support around the base of the damper, lateral reinforcement was applied intensively in the upper and lower parts of the H-section steel in addition to shear reinforcement.

In the element test, 1/2-scale specimens were used that represented the bottom half of the pillar type damper shown in Fig. 1. The H-section steel in the upper part of the specimen simulated the hysteretic damper and was embedded into the RC. The H-section steel had yield strength of 2.5 times the bending moment and 1.5 times the shear force that acted when the flexural strength was reached in RC support. In specimen No. 1, the H-section steel was simply embedded into the RC support. Specimens No. 2 through 6 were modified for transferring the moment. In specimen No. 2, a base plate was attached to the H-section steel at the top end of the RC support. Only four main reinforcing bars near the flanges on both sides of the H-section steel were made to penetrate the plate and anchored to the plate by nuts. In specimen No. 3, a base plate was installed at the bottom end of the H-section steel. In specimen No. 4 and 5, stud bolts were installed on the flanges of the H-section steel. In specimen No.5, based on assumption that the bending moment would be resisted only by the stud bolts, the number of stud bolts was determined so that shear strength of stud bolts exceeded the shear forced that acted when the flexural strength was reached in RC support. The number of stud bolts in specimen No. 4 was set at 1.5 times that in specimen No. 5 to increase stiffness. In specimen No. 6, base plates were installed only at the bottom ends of flanges of H-section steel.

Table 1 Details of specimens (*:top stab)

Specimen code	Steel cross section	Base plate	Stud bolt	Transverse reinforcement (pw%)	Lateral reinforcement			Concrete strength (MPa)
					Top	Bottom	Yield stress (MPa)	
No.1	300x125 x 9x12 (B x D x t1 x t2)	-	without	2-U9@60 (1.21)	6-U9	4-U9	1329	35.1
No.2		top(t=12)		2T10@70 (1.17)	6-T10	4-T10	820	36.8
No.3		bottom(t=19)		2D6@100 (0.37)	10-D10	4-D10	351(316:D6)	37.1
No.4		-	12-φ13	2UHD6@34 (1.07)	10-UHD10	4-UHD10	829:UHD10 (699:UHD6)	38.6
No.5		-	12-φ13					41.4
No.6		bottom(t=19)	without					42.4
No.7	300x100 x6.5x9	-	12-φ13	4-RB6.2@40 (1.33)	6-RB6.2	6-RB6.2	822	42.8(43.9*)
No.8		-		4-RB6.2@35 (1.71)	6-RB6.2	-	872	34.9(38.1*)

For transferring the moment in the specimen in the member test, stud bolts were installed on the flanges, which had contributed to high structural performance in the element test. Specimens of 1/2 scale were used in the element test. The H-section steel at the center of the specimen represented the hysteretic damper and was embedded into the RC support to a depth of 300 mm. At the concrete encased steel, stud bolts were installed on the flanges. The web was cut out at the center of the damper. Low-yield-strength steel LY100 (yield stress: 100 MPa) and LY225 (yield stress: 225 MPa) were applied in specimen No. 7 and 8, respectively using a fillet weld. Table 2 lists the mechanical properties of steel. Concrete strength was 34.9 to 42.8 (MPa) during the test.

Table 2 Mechanical properties of steel

Thickness of steel	Yield stress (MPa)	Tensile strength (MPa)
PL9(No.1 to No.6)	409	516
PL12(No.1 to No.6)	349	524
PL6.5(No.7)	330	465
PL6.5(No.8)	281	428
PL9(No.7)	429	520
PL9(No.8)	326	450

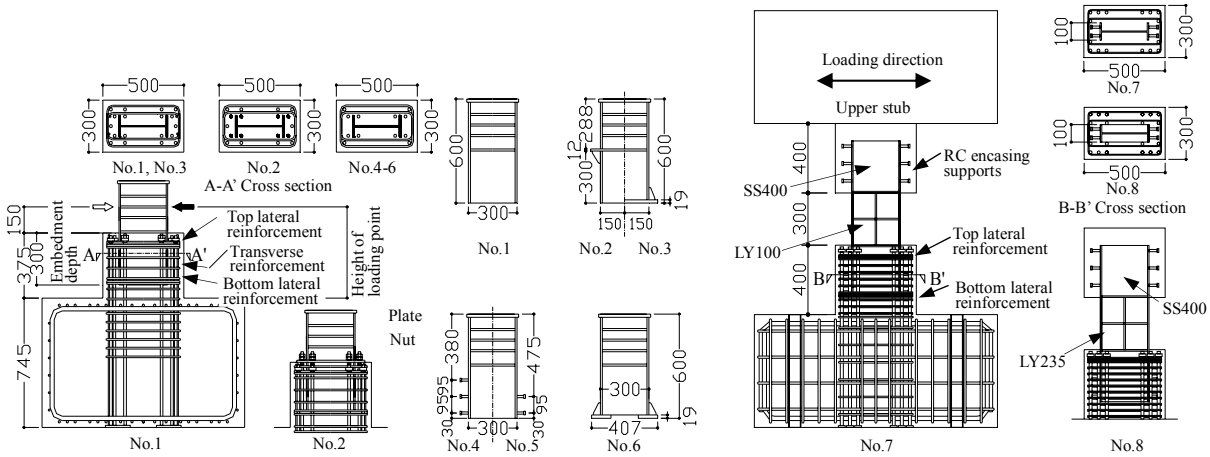

Figure 2 Details of specimen

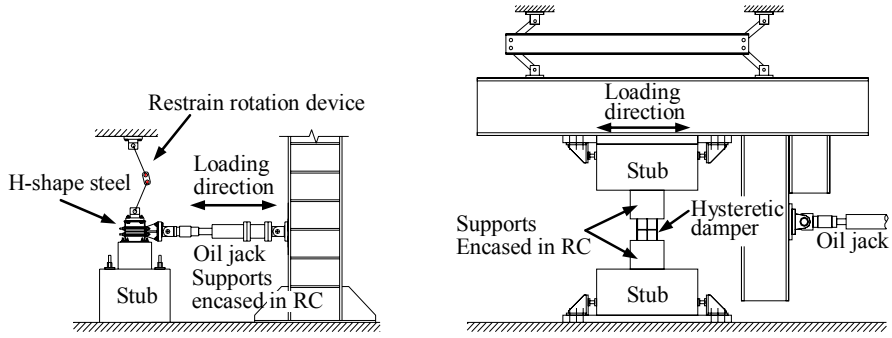

(a) Element test (b) Member test

Figure 3 Test set-up

3.2. Testing procedure and instrumentation

The test set-up is shown in Fig. 3. In the element test, the test set-up was designed to subject the test specimen to cyclic lateral load. Using bolts, the bottom stub was securely tied to reaction frame. Cyclic loading was applied twice each at an drift angle of the member *R* (lateral displacement at the point of loading divided by height of the loading point) of 0.1, 0.2, 0.3, 0.4 and 0.5%, and once each at *R* of 0.75, 1.0, 1.5 and 2.0%.In the member test, the loading system loaded the test specimens in a double-bending moment condition, with the point of inflection occurring at the mid-height of the specimen. Cycles of loading was once each at a drift angle of member *R* (lateral displacement divided by inner size) of 0.1 and 0.5%, twice each at *R* of 0.3, 0.5, 0.75, 1.0 and 1.5%, and

once each at R of 0.75, 2.0 and 3.0%. No axial load was applied.

Lateral load were measured using load cells placed with oil jack. Measurements were displacement of specimen in the horizontal direction, drift angle and lateral deformation in the RC support, and pullout of H-section steel. Strain gauges were mounted to the main reinforcement, shear reinforcement and lateral reinforcement in the RC support, and on the flanges and web of H-section steel for measurement.

4. RESULTS OF EXPERIMENTS

4.1. Visual observation and measurements

Figure 4 shows the lateral load-displacement behavior of each specimen.

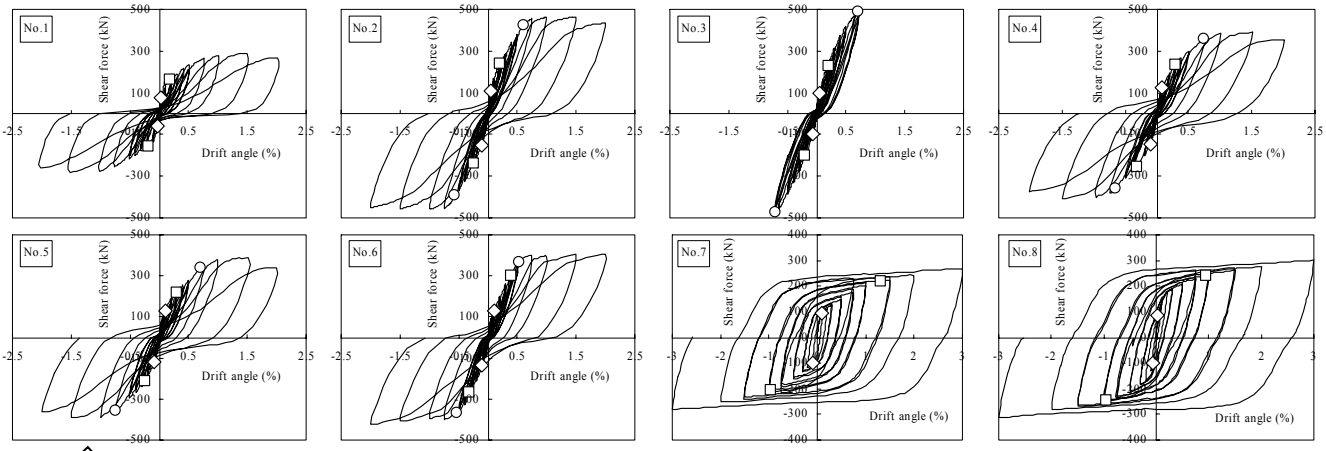

Note: ◇=first flexural crack; □ =first shear crack; ◯ = flexural yielded strength

Figure 4 Lateral load-displacement responses

4.1.1 Element test

Shear cracking occurred in specimen No. 1 earlier than in any other specimens and stiffness decreased considerably. The maximum strength was reached at R = 1.5%, and shear failure occurred before the yielding of main reinforcement. In specimen No. 2, the main reinforcement yielded at R = 0.8%, the maximum strength was reached, and load-carrying capacity decreased after the width of the shear crack expanded. In specimen No. 3, the main reinforcement yielded at R = 0.75% and loading was discontinued because of the restrictions of jack capacity. In specimen No. 4 and 5, the main reinforcement yielded at R = 0.7%, the maximum strength was reached at R = 1.5%, and load-carrying capacity decreased after the width of the shear crack expanded. In specimen No. 6, the main reinforcement started yielding at R = 0.5%, the maximum strength was reached at R = 2.0%, and load-carrying capacity decreased after the width of the shear crack expanded.

In specimen No. 1 in which H-section steel was simply embedded into RC, the ratio of the deformation due to the pullout of the H-section steel to the horizontal displacement a loading point was much higher than in any other specimen. The pullout deformation was divided by the horizontal displacement a loading point to obtain the pullout ratio. The pullout deformation was obtained by multiplying the height between the loading point and top of RC support, by the rotation angle of H-section steel which occurred by pullout of the H-section steel from RC support. In specimen No. 2 in which main reinforcement was anchored to the base plate at the top end of the RC support by nuts, the H-section steel was hardly pulled out in the initial stages, but the ratio of deformation due to the pullout of the H-section steel increased as the drift angle of the member increased. In specimen No. 5 with stud bolts and in specimen No. 6 with a base plate, the ratio of deformation due to the pullout of the H-section steel was constantly at a low level throughout the test.

4.1.2 Member test

Cracks occurred at the bottom of the flange at the top and bottom joints between the damper and RC support, and flexural cracks occurred at the bottom of RC. Subsequently, shear cracks occurred at the RC support. The web of the damper with low-yield-strength steel yielded due to shear at R = 0.1% in specimen No. 7, and at R =0.2% in specimen No. 8. After the shear yielding, load-carrying capacity was increasing both in specimen No. 7 and 8. No deterioration of strength was observed at R = 3.0%. Neither main reinforcement nor shear reinforcement yielded in both specimens.

4.2 Evaluation of data obtained in experiments

4.2.1 Load transfer mechanism

Load transfer mechanism is proposed in this section based on the shear acting on the steel. Fig. 5 shows the vertical distribution of moments carried by the steel. Based on Bernoulli-Euler hypothesis, the moment of each point was calculated using the strain in the flanges of H-section steel, and moment was divided by moment at bottom end of the RC support for comparison. The moment carried by specimen No. 2 was reduced greatly at the head of RC because the main reinforcement was connected to the base plate. In specimen No. 3 and 6 with a base plate at the bottom end of the steel, the steel carried at a constant ratio the moment applied in the RC support. The moment carried by other specimens with stud bolts gradually decreased from the joint between the steel and RC to the end of the steel.

Fig. 6 shows the vertical distribution of shear carried by the steel. The shear carried by the steel linearly decreased to the bottom end as shown in the distribution of moments. Much greater shear acted at the bottom of the H-section steel in specimen No. 1 than in other specimens.

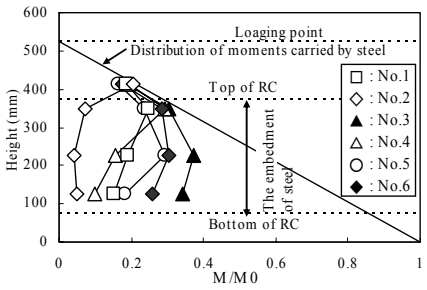

Figure 5 Moment bearing ratio of H-shape steel

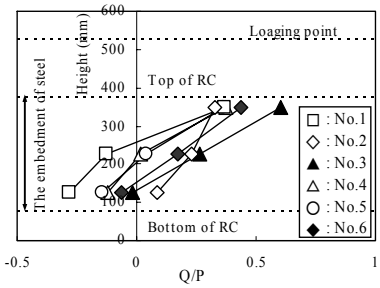

Figure 6 Shear bearing ratio of H-shape steel

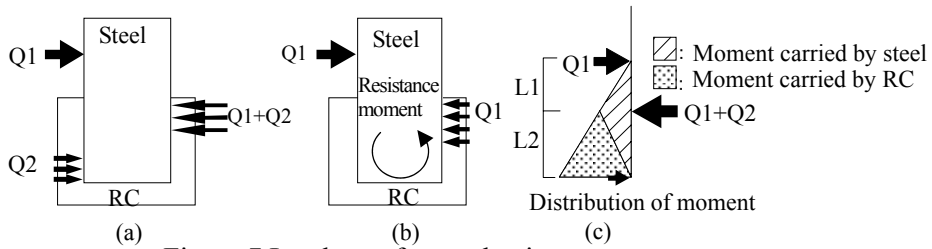

Figure 7 Load transfer mechanism

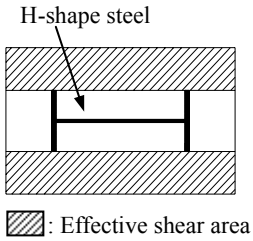

Figure 8 Effective shear area

Fig. 7 (a) and (b) show two models of load transfer mechanism in the section where H-section steel was embedded. In the case where H-section steel was simply embedded into the specimen, it was necessary for a couple of reactions of concrete on both sides to resist the moment. Then, the shear force that was applied to the RC would be *Q1 + Q2*, greater than *Q1*, the shear force that was applied to the H-section steel in the upper part of specimen. Based on the distribution of moments shown in Fig. 7 [3], the shear forced *Q1+Q2* can be calculated by *Q1 (1+L1/L2)*. For the H-section steel with a based plate at the bottom end that resisted the moment, the load transfer mechanism is shown in Fig.7 (b). The shear force that acted on the RC was identical

with shear force *Q1* that was applied to the H-section steel in the upper part of the specimen. Fig. 5 and 6 suggest that the load transfer mechanism of specimen No. 1, No.2, 3 and 6 were similar to model (a), model (b), respectively. The load transfer mechanism of specimens with stud bolts is a mixture of the mechanism of model (a) and model (b).

4.2.2 Load-carrying capacity

Tables 3 and 4 compare experimental results of the maximum shear forces acting on the specimens with calculations. Experimental result 1 is the shear force acting on the specimen (load applied using the jack). Experimental result 2 is the shear force acting on the RC support calculated based on Fig. 7 (c). Calculation 1 is the shear force for the reinforcement at the extreme edge that yielded, which was obtained from the moment-curvature relationship in the cross section at the bottom end of the RC support. Calculation 2 is the shear strength obtained by A-method [4]. As shown in Fig. 8, the effective area resisting to the shear force was assumed.

The ultimate shear strengths of dampers in specimen No. 7 and 8 used in the member test Q_{du} were obtained using an equation [5]. The strength at the joint between the stud bolt and steel was evaluated using a shear strength equation for stud connectors. Equations 4.1 and 4.2 have been presented for calculating the shear strength of stud connectors [6]. Equation 4.1 expresses the strength determined by bearing strength of concrete in contact with the stud connector. Equation 4.2 expresses the strength determined by concrete cone failure based on the assumption of the failure area shown in Fig. 9.

$$Q_{std} = n \cdot 0.5_{sc} a \sqrt{F_c \cdot E_c} \tag{4.1}$$

$$Q_{anc} = \sqrt{F_c} \cdot A_c \tag{4.2}$$

Where, n is the number of stud bolts, $_{sc}a$ is the cross-sectional area of stud bolt, F_c and E_c are compressive strength and Young's modulus of concrete and A_c is the effective projected area of concrete cone failure.

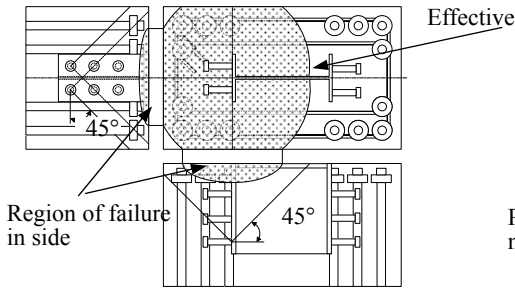

Figure 9 Effective projected area of concrete cone failure

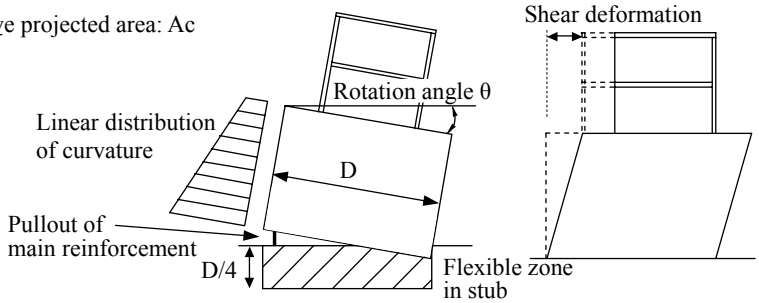

(a) Bending deflection (b) Shear deformation

Figure 10 Schematic illustration of deformation model

For specimen No. 1, experimental result 2 and calculation 2 show a good correspondence. It is supposed that the RC support failed in shear before the main reinforced yielded. In specimen No.2 through 6, experimental result 2 substantially exceeded calculation 2. It was, however, thought that the acting force on specimen was equal to the experimental result 1. The yielding of main reinforcement may have preceded shear failure because the shear strength was greater than flexural strength. In specimen No. 3, however, shear strength ratio was about 1.0. Specimen No. 7 and 8 were designed so that the flexural and shear strength in the RC support would considerably exceed the shear strength of the damper. The shear strength applied to the RC support was expected to be much greater than shear strength of the specimen (Fig. 7). Adequate shear strength should be secured necessary for flexural strength in the RC support. The experimental results clearly show that the increase of strength of the damper with low-yield-strength steel owing to strain hardening was significant. In structural design, RC support should be provided with sufficient resistance. Designing the specimen so that the crack strength could exceed the

strength of the damper is difficult. It was necessary to prevent cracks from occurring at the base of a concrete-encased pillar type hysteretic damper.

The strength at the joint between the stud bolt and steel was evaluated. The strength of the stud bolt Q_{anc} obtained by Eqn.4.2 was smaller than that obtained by Eqn.4.1 for all the specimens. The strength of stud bolt obtained by Eqn.4.2 was greater than the maximum strength. It was therefore assumed that no failure occurred. This suggests that the Eqn.4.2 should be used for calculating the shear strength of the stud bolt.

Table 3 Test results

Specimen code	Maximum shear force (kN)						
	Experiment 1 Q1(kN)	Experiment 2 Q1(1+L1/L2)	Calculated 1	Calculated 2	Exp.1/Cal.1	Exp.1/Cal.2	Exp.2/Cal.2
No.1	290	528	475	526	0.61	0.55	1.00
No.2	462	842	475	537	0.97	0.86	1.57
No.3	490	893	476	431	1.03	1.14	2.07
No.4	391	712	344	544	1.14	0.72	1.31
No.5	389	709	342	562	1.14	0.69	1.26
No.6	408	743	345	568	1.18	0.72	1.31

Table 4 Test results

Specimen code		Experiment (kN)			Calculated (kN)									
					RC encasing supports						Damper			
		Q_{mc}	Q_{sc}	Q_{max}	${}_cQ_{mc}$	${}_cQ_{sc}$	Q_{mu}	Q_{su}	Q_{std}	Q_{anc}	Q_{dmy}	Q_{dmu}	Q_{dy}	Q_{du}
No.7	positive	94	225	268	106	196	467	716	848	445	664	664	68	277
	negative	-100	-205	-280										
No.8	positive	86	241	302	101	174	548	600	735	401	545	579	155	301
	negative	-100	-244	-313										

Notes: Q_{mc}= flexural crack strength; Q_{sc}= shear crack strength; Q_{mu}= flexural strength; Q_{su} = ultimate shear strength; Q_{max}= maximum load; Q_{dmy}= flexural yield strength Q_{dmu}= flexural ultimate strength; Q_{dsy}= shear yield strength; Q_{dsu}= shear ultimate strength

5. HYSTERESIS MODEL IN THE REINFORCED CONCRETE SUPPORT

Models of the hysteretic characteristics were proposed based on the results of the element test except for specimen No. 1 subject to shear failure. H-section steel was not embedded to the bottom end of the RC support. The flexural behavior of the RC support seemed to be determined by the bar arrangement at bottom of the RC support. Then, the characteristics of bending in the RC support was proposed using a tri-linear model with flexural cracking and the yield of main reinforcement as singular points considering only the cross section of the RC. The yield deformation was calculated by obtaining the yield curvature from the moment-curvature relationship in the RC cross section, based on the curvature distribution in Fig. 10. Deformation due to the pullout of main reinforcement was evaluated based on reference [7] and added. Here, a flexible zone was created above the stub abutment (Fig. 10) and its elastic deformation was also considered. The shear characteristics were obtained by calculating the elastic stiffness and stiffness after shear cracking based on the method of performance evaluation of beam-yielding type mechanism [7] using the cross-sectional area carrying the shear (Fig. 8).

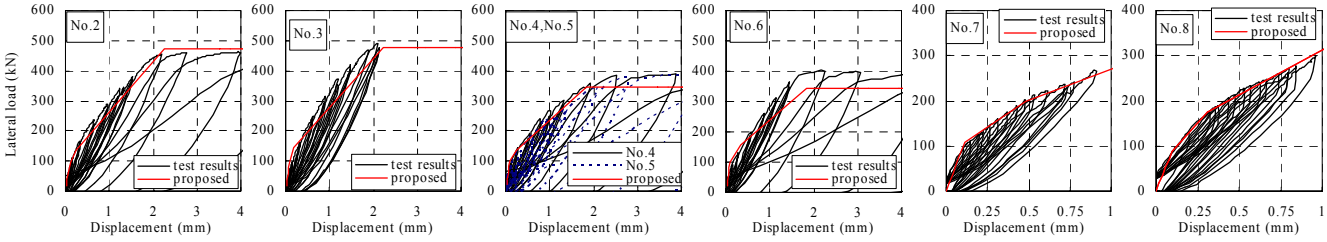

Figure 11 Comparison of experimental and analytical results

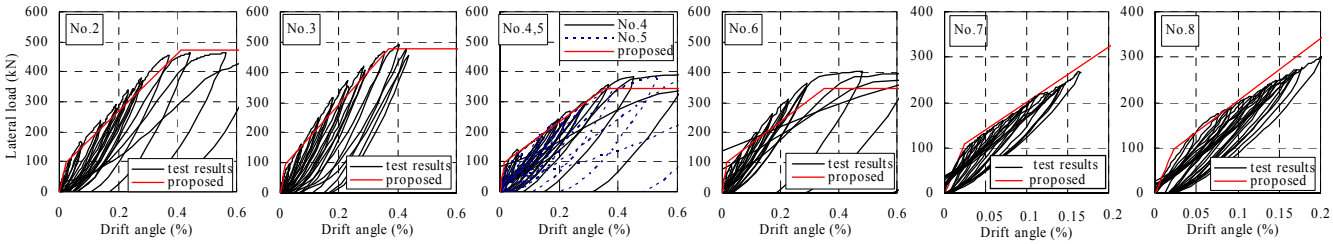

Figure 12 Comparison of experimental and analytical results

Figure 11and 12 shows a comparison between results obtained using the proposed model and experimental result of rotation angle and lateral deformation on the top end of the RC support. The results obtained using proposed model corresponds to the experimental results for specimen No.2, 4, 5, 7 and 8. Thus, the hysteresis characteristics in the RC support can be determined by the flexural and shear deformations in the RC support. In specimen No. 3 and 6 with a base plate at the bottom end of the H-section steel, however, post-cracking stiffness in the experiment was slightly higher than that obtained using models. This suggests that the H-section steel carried the moment. The shear force at the yielding of main reinforcement generally corresponds to the experimental results.

6.CONCLUSIONS

Based on the test results and the discussions above, following conclusions can be drawn:

1. In specimen No. 1 with H-section steel simply embedded into the RC at the base of the damper, shear failure was occurred before the yielding of main reinforcement in the RC support, and the strength greatly decreased. The other specimens behaved stably until they yielded. A member test revealed that the increase of strength of the damper with low-yield-strength steel was significantly and that providing sufficient allowance in the design of the RC support was important.
2. The joint between the stud bolt and steel should be designed so that the shear strength that is determined by the concrete cone failure may exceed the load-carrying capacity of the damper.
3. The proposed model of hysteresis characteristics in the RC support can be determined by the flexural and shear deformations in the RC support. The proposed model could be specified that were in good agreement with experimental results. In the case where a base plate was installed at the bottom end of the H-section steel, calculation results were conservative with respect to the post-cracking stiffness and strength. This issue is unclear and more studies are needed.
4. Smaller deformations of the RC support were observed for specimen using the simple joint method. This suggests that proposed method of joint had performance for damper enough.

REFERENCES

1. Yasuda,S., Tokita,T., Kimura,M., Hara,T., Narihara,H. And Soya, K., “Development of Hysteretic Damper using Low Yield Stress Steel for R/C Structures”, Summaries of Technical Papers of Annual Meeting Architectural Institute of Japan, 2001, C-1, 1073-1074. (in Japanese)

2. Fuchigami, K., Tomatsuri, H. and Okina, Y., ”Development of Low-yield-point Hysteretic Steel Damper for Seismic Response Control reinforced concrete building” Summaries of Technical Papers of Annual Meeting Architectural Institute of Japan, 2001, C-2, 783-784. (in Japanese)

3. The Building Center of Japan, ”Guidelines to Structural Calculation under the Building Standard Low”, *The Building Center of Japan*,,1997 (in Japanese)

4. Architectural Institute of Japan, “AIJ Structural Design Guidelines for Reinforced Concrete Buildings”, *Architectural Institute of Japan*, 1994

5. Matsuura, T., Ito, Y. and Inai, E., “Structural Performance of Energy Absorbing Devices Using Low Yield Strength Steel, Part2 test results and discussion”, Summaries of Technical Papers of Annual Meeting Architectural Institute of Japan, 2001, C-2, 611-612. (in Japanese)

6. Architectural Institute of Japan, “Design Recommendations for Composite Constructions”, *Architectural Institute of Japan*, 1985 (in Japanese)

7. Architectural Institute of Japan, “Guideline for Performance Evaluation of Earthquake Resistant Reinforced Concrete Buildings”, *Architectural Institute of Japan*, 2004 (in Japanese)